

Autosomal dominant immune dysregulation syndrome in humans with *CTLA4* mutations

Desirée Schubert^{1,2,15}, Claudia Bode^{1,15}, Rupert Kenefeck^{3,15}, Tie Zheng Hou^{3,15}, James B Wing⁴, Alan Kennedy³, Alla Bulashevskaya¹, Britt-Sabina Petersen⁵, Alejandro A Schäffer⁶, Björn A Grüning⁷, Susanne Unger¹, Natalie Frede¹, Ulrich Baumann⁸, Torsten Witte⁸, Reinhold E Schmidt⁸, Gregor Dueckers⁹, Tim Niehues⁹, Suranjith Seneviratne³, Maria Kanariou¹⁰, Carsten Speckmann¹, Stephan Ehl¹, Anne Rensing-Ehl¹, Klaus Warnatz¹, Mirzokhid Rakhmanov¹, Robert Thimme¹¹, Peter Hasselblatt¹¹, Florian Emmerich¹², Toni Cathomen^{1,12}, Rolf Backofen⁷, Paul Fisch¹³, Maximilian Seidl¹³, Annette May¹³, Annette Schmitt-Graeff¹³, Shinji Ikemizu¹⁴, Ulrich Salzer¹, Andre Franke⁵, Shimon Sakaguchi⁴, Lucy S K Walker^{3,15}, David M Sansom^{3,15} & Bodo Grimbacher^{1,3,15}

The protein cytotoxic T lymphocyte antigen-4 (CTLA-4) is an essential negative regulator of immune responses, and its loss causes fatal autoimmunity in mice. We studied a large family in which five individuals presented with a complex, autosomal dominant immune dysregulation syndrome characterized by hypogammaglobulinemia, recurrent infections and multiple autoimmune clinical features. We identified a heterozygous nonsense mutation in exon 1 of *CTLA4*. Screening of 71 unrelated patients with comparable clinical phenotypes identified five additional families (nine individuals) with previously undescribed splice site and missense mutations in *CTLA4*. Clinical penetrance was incomplete (eight adults of a total of 19 genetically proven *CTLA4* mutation carriers were considered unaffected). However, CTLA-4 protein expression was decreased in regulatory T cells (T_{reg} cells) in both patients and carriers with *CTLA4* mutations. Whereas T_{reg} cells were generally present at elevated numbers in these individuals, their suppressive function, CTLA-4 ligand binding and transendocytosis of CD80 were impaired. Mutations in *CTLA4* were also associated with decreased circulating B cell numbers. Taken together, mutations in *CTLA4* resulting in CTLA-4 haploinsufficiency or impaired ligand binding result in disrupted T and B cell homeostasis and a complex immune dysregulation syndrome.

Adaptive immune responses must balance the response against foreign antigens with the need to avoid damage to host tissue. Inefficient activation of the immune response results in pathology due to infections, whereas overactivation may drive an autoimmune response. It might be expected that distinct genetic mutations underlie these apparently opposite outcomes, yet, paradoxically, it is well recognized that autoimmunity and immunodeficiency can manifest concurrently in the same individuals¹.

Common variable immunodeficiency (CVID) is the most frequent primary immunodeficiency in humans characterized by low immunoglobulin levels, recurrent upper respiratory tract infections and impaired vaccination responses^{2,3}. In many patients, CVID presents as an immune dysregulation syndrome with autoimmunity, granulomatous disease,

enteropathy, and malignancy⁴. The majority of familial CVID cases present an autosomal dominant pattern of inheritance, yet disease penetrance may appear incomplete owing to the late onset of symptoms⁵. Dominant mutations causing CVID have been found in *NFKB2* (ref.6), and some patients with activating *PIK3CD* mutations present with a CVID-like phenotype⁷. Still, most autosomal dominant mutations causing CVID or increasing the disease risk remain to be identified.

The mammalian immune system contains self-reactive T cells, which are controlled by forkhead box P3-positive (FOXP3⁺) T_{reg} cells^{8,9}. Accordingly, T_{reg} deficiency caused by mutations in *FOXP3* leads to an aggressive autoimmune syndrome termed IPEX (immune dysregulation polyendocrinopathy X-linked)¹⁰. In mice, deficiency of CTLA-4 results in a lethal autoimmune phe-

¹Center for Chronic Immunodeficiency, University Medical Center Freiburg, Freiburg, Germany. ²Spemann Graduate School of Biology and Medicine, Freiburg University, Freiburg, Germany. ³University College London Institute of Immunity and Transplantation, Royal Free Campus, London, UK. ⁴World Premier International Immunology Frontier Research Center, Osaka University, Osaka, Japan. ⁵Institute of Clinical Molecular Biology, Christian-Albrechts-University of Kiel, Kiel, Germany. ⁶National Library of Medicine, National Institutes of Health, Bethesda, Maryland, USA. ⁷Department of Computer Science, University of Freiburg, Freiburg, Germany. ⁸Department of Pediatric Pulmonology, Allergy and Neonatology, Hannover Medical School, Hannover, Germany. ⁹HELIOS Children's Hospital, Krefeld, Germany. ¹⁰Department of Immunology and Histocompatibility, "Aghia Sophia" Children's Hospital, Athens, Greece. ¹¹Clinic for Internal Medicine 2, University Medical Center Freiburg, Freiburg, Germany. ¹²Institute for Cell and Gene Therapy, University Medical Center Freiburg, Freiburg, Germany. ¹³Department of Pathology, University Medical Center Freiburg, Freiburg, Germany. ¹⁴Division of Structural Biology, Kumamoto University, Kumamoto, Japan. ¹⁵These authors contributed equally to this work. Correspondence should be addressed to B.G. (bodo.grimbacher@uniklinik-freiburg.de).

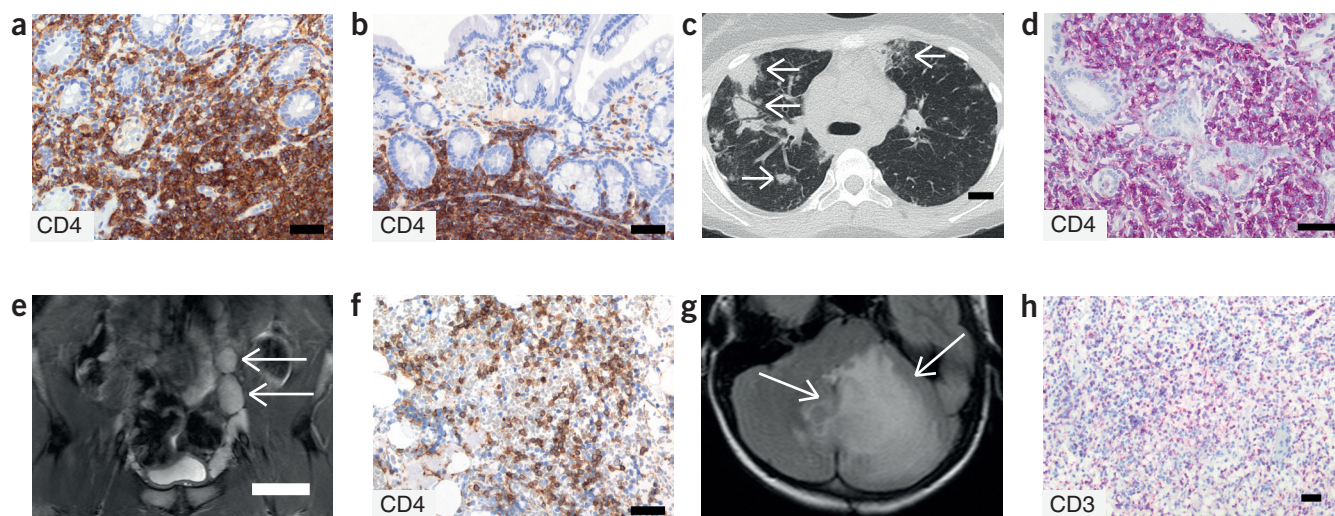


Figure 2 Tissue infiltration and lymphadenopathy in patients with *CTLA4* mutations. (a,b) Duodenal biopsies from patient B.II.4 (a) and A.III.3 (b) stained for CD4. (c) High-resolution chest computed tomography scan of the lungs from patient E.II.3. Arrows point to granulomatous-lymphocytic infiltration in both lungs. (d) Pulmonary lymphoid fibrotic lesions stained for CD4 in pulmonary biopsy from patient E.II.3. (e) Magnetic resonance imaging (MRI) of the pelvic area of patient A.III.3 with two enlarged lymph nodes (arrows) measuring up to 4 cm. (f) Bone marrow biopsy from patient B.II.4 stained for CD4. (g) MRI of gadolinium-enhanced lesion (arrows) in the cerebellum of patient A.III.1. (h) Resected cerebellar lesion from patient A.III.1 stained for CD3. Scale bars, 50 μ m (a,b,d,f,h), 20 mm (c) and 50 mm (e).

CTLA4 mutation; for three patients (A.II.8, B.II.2 and B.III.2) no genomic DNA was available as they had died before this study) and eight carriers (Fig. 1a). Seven of the 14 patients fulfilled the diagnostic criteria of CVID. A splice-site mutation (family B) and a mutation in the start codon (family F), comparable to the nonsense mutation in family A, were predicted to result in haploinsufficiency due to a lack of CTLA-4 expression from one allele (Fig. 1b). Three distinct missense mutations (families C–E) affected conserved amino acids in the extracellular domain (Fig. 1b) and were predicted to interfere with ligand binding or CTLA-4 stability (Supplementary Fig. 2). Table 1 contains a summary of the clinical findings of all individuals with CTLA-4 deficiency, and details are given in Supplementary Note 2 and in Supplementary Table 1.

Lymphocytic organ infiltration and lymphadenopathy

Ctla4^{-/-} mice die from CD4⁺ T cell-dependent organ infiltration^{11,12,29}. Investigating the clinical symptoms of patients with CTLA-4 mutations, we

confirmed extensive CD4⁺ T cell infiltration in a number of organs including the intestines (Fig. 2a,b), lungs (Fig. 2c,d), bone marrow (Fig. 2f), central nervous system (Fig. 2g,h) and kidneys (Supplementary Note 2). We also found lymphadenopathy (Fig. 2e) and hepatosplenomegaly in these individuals (Supplementary Note 2).

Activated T cells and reduced B cells in peripheral blood

Where sufficient blood samples were available, we carried out detailed immunological investigations in families A–D. Consistent with the observed lymphoproliferation and lymphocytic tissue infiltration, analysis of peripheral blood revealed evidence of increased T cell activation in *CTLA4*^{+/-} carriers and affected individuals, as assessed by reduced levels of CD4⁺CD45RA⁺ naive T cells (Fig. 3a). Although the affected individuals generally had lymphopenia in the periphery (Supplementary Table 2), the ratio of CD4⁺ to CD8⁺ T cells was in the normal range (Supplementary Fig. 3a). All symptomatic patients with *CTLA4* mutations except B.II.1 had reduced levels of at

Table 1 Clinical phenotype of patients with *CTLA4* mutations

Clinical manifestations	Patients	Frequency
Diarrhea/enteropathy	A.II.5, A.II.8, A.II.9, A.III.1, A.III.3, B.II.1, B.II.2, B.II.4, C.II.4, E.II.3, F.II.2	11/14 (78%)
Hypogammaglobulinemia	A.II.5, A.II.8, A.II.9, A.III.1, A.III.3, C.II.3, B.III.2, D.II.1, E.II.3, F.II.2	10/13 (76%)
Granulomatous lymphocytic interstitial lung disease	A.II.8, A.II.9, A.III.3, B.II.4, B.III.2, C.II.3, D.II.1, E.II.3	8/12 (66%)
Respiratory infections ^a	A.II.5, A.II.8, A.II.9, B.II.4, B.III.2, C.II.3, E.II.3, F.II.2	8/14 (57%)
Organ infiltration (bone marrow, kidney, brain, liver)	A.II.9, A.III.1, A.III.3, B.II.2, B.II.4, C.II.3, D.II.1	7/14 (50%)
Splenomegaly	A.II.5, A.II.9, A.III.3, C.II.3, D.II.1, E.II.3	6/12 (50%)
Autoimmune thrombocytopenia	A.III.1, A.III.3, C.II.3, E.II.3, F.II.2	5/14 (35%)
Autoimmune hemolytic anemia	C.II.3, D.II.1, E.II.3, F.II.2	4/14 (28%)
Lymphadenopathy	A.III.3, C.II.3, D.II.1, E.II.3	4/14 (28%)
Psoriasis and other skin diseases ^b	A.III.1, B.II.1, B.II.2	3/14 (21%)
Autoimmune thyroiditis	A.II.5, D.II.1	2/13 (15%)
Autoimmune arthritis	A.II.5, A.III.1	2/14 (14%)
Solid cancer	B.II.4	1/14 (7%)

Denominators vary between rows because some deceased patients had not been evaluated for all clinical manifestations. Details are shown in Supplementary Table 1.

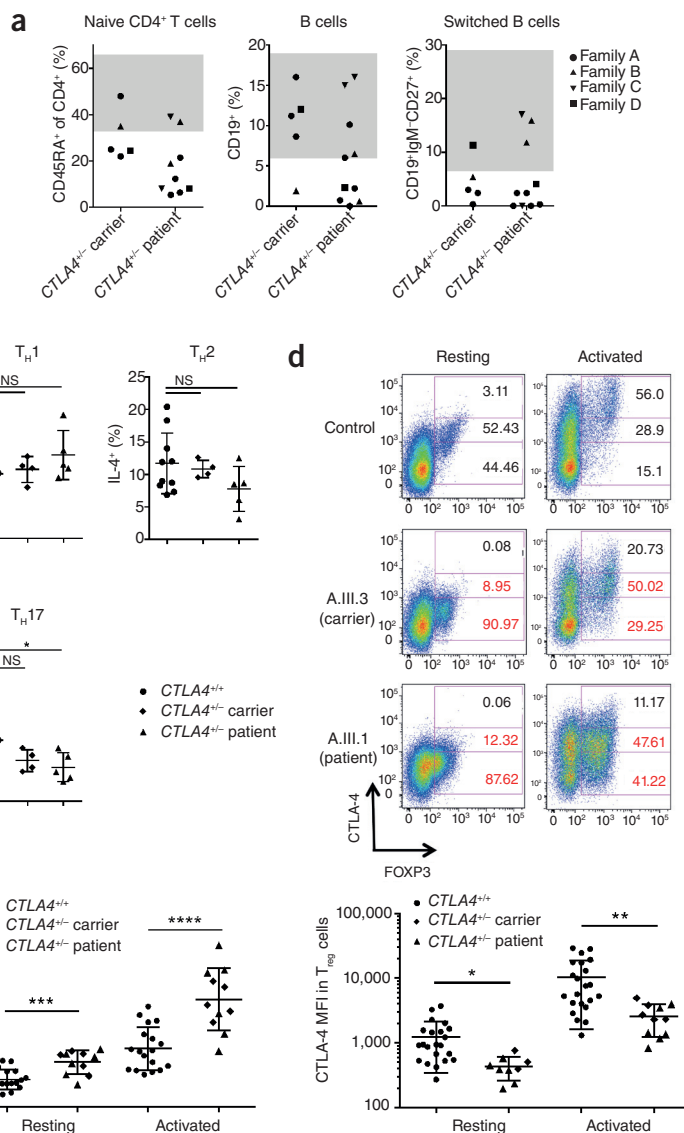
^aUpper and lower respiratory tract infections. ^bDetails in Supplementary Note 2.

Figure 3 Impact of *CTLA4* heterozygosity on T and B cells. **(a)** Percentage of naive CD4⁺CD45RA⁺ T cells, CD19⁺ B cells and CD19⁺IgM-CD27⁺ switched memory B cells in the peripheral blood of *CTLA4*^{+/-} carriers and patients. Gray background indicates normal range. **(b)** Proportion of IFN- γ , IL-4- and IL-17-expressing CD3⁺CD4⁺CD45RO⁺ T cells after stimulation of PBMCs with phorbol 12-myristate 13-acetate and ionomycin from healthy *CTLA4*^{+/+} subjects, *CTLA4*^{+/-} carriers and *CTLA4*^{-/-} affected individuals. **(c)** Percentage of FOXP3⁺ T_{reg} cells among CD4⁺ T cells in the peripheral blood under resting (*ex vivo*) conditions or following activation (with beads coated with CD3- and CD28-specific antibodies). **(d)** Representative (11 mutation carriers and 22 controls) flow cytometry plots (top) and quantification (bottom) of CTLA-4 expression in CD4⁺FOXP3⁺ cells under resting and activated conditions. Numbers in quadrants show percentage of CTLA-4-high (top), CTLA-4-intermediate (middle) and CTLA-4-low (bottom) cells within the FOXP3⁺ population. MFI, mean fluorescence intensity. Plots in **b–d** show the mean \pm s.d.; each dot represents one individual. *P* values were determined by Student's *t*-test. **P* \leq 0.05; ***P* \leq 0.01, ****P* \leq 0.001, *****P* \leq 0.0001. NS, not significant.

least one immunoglobulin isotype (Supplementary Table 2); seven out of ten patients had low proportions of CD19⁺ B cells (Fig. 3a) and low numbers of switched (IgM-CD27⁺) memory B cells (Fig. 3a). Additional characterization of the lymphocyte compartment is shown in Supplementary Figure 3a and Supplementary Table 2. In five out of six patients who were monitored over at least 2 years, we observed a progressive loss of CD19⁺ B cells over time (Supplementary Fig. 4). *In vitro* re-stimulation of T cells from affected individuals did not suggest a bias toward T helper type 1, 2 or 17 differentiation (Fig. 3b). As some affected individuals showed T cell infiltrates into multiple organs, we were interested in whether their T cells had a polyclonal distribution of T cell receptors (TCRs). We observed that A.II.5 had an oligoclonally expressed T cell receptor β , γ and δ repertoire in the peripheral blood, whereas A.III.3 had a normal distribution (Supplementary Fig. 3b). The oligoclonal T cell repertoire of A.II.5 was confirmed by TCR spectratyping (Supplementary Fig. 3c).

CTLA-4 expression is reduced in T_{reg} cells

Given the role of CTLA-4 in T_{reg} cell function¹⁹, we analyzed the T_{reg} cell compartment in symptomatic individuals or healthy carriers bearing *CTLA4* mutations. The frequency of FOXP3⁺ T_{reg} cells within the CD4⁺ T cell compartment was higher in individuals with a heterozygous *CTLA4* mutation compared to healthy *CTLA4*^{+/+} controls (Fig. 3c). Consistent with this, both homozygous³⁰ and heterozygous loss of *Ctla4* in mice (Supplementary Fig. 5) are associated with an increased frequency of T_{reg} cells. To investigate the impact of the mutations on CTLA-4 protein expression, we carried out intracellular staining for CTLA-4. CTLA-4 expression was reduced in FOXP3⁺ T cells from all individuals with *CTLA4* mutations compared with healthy *CTLA4*^{+/+} control cells (Fig. 3d), a deficit that was more pronounced following T cell activation. Thus, in healthy control subjects, activated T_{reg} cells expressed levels of CTLA-4 in excess of those in the FOXP3⁻ conventional T cell population. In contrast, in individuals with *CTLA4* mutations, the expression of CTLA-4 in activated T_{reg} cells was similar to the expression in activated conventional T cells. Taken together, these data



indicate that two functional *CTLA4* alleles appear necessary to drive the high levels of protein required in activated T_{reg} cells.

Ligand binding and capture is impaired by *CTLA4* mutations

To investigate CTLA-4 function, we tested the ability of T_{reg} cells to perform transendocytosis²⁵ (see Supplementary Fig. 6 for assay design). We cocultured stimulated CD4⁺FOXP3⁺ T cells with CD80-GFP-expressing Chinese hamster ovary (CHO) cells and analyzed their ability to capture ligand by flow cytometry (Fig. 4a). T_{reg} cells from healthy *CTLA4*^{+/+} individuals transendocytosed efficiently with 10–25% becoming positive for CD80-GFP; this percentage was reduced to only 2–3% in individuals bearing *CTLA4* mutations, indicating a deficit in ligand capture. Transendocytosis of CD80 was inhibited when a blocking CTLA-4-specific antibody was added to cell cultures, confirming that the ligand capture was CTLA-4 dependent (Fig. 4a).

To study the impact of *CTLA4* point mutations in the absence of co-expressed wild-type protein, we cloned the *CTLA4* mutants identified in our patients, expressed these in CHO cells and used these cells for soluble CD80 ligand uptake assays (Fig. 4b). We assessed protein expression by permeabilizing the cells and using an antibody that recognizes an epitope in the cytoplasmic domain of CTLA-4. This avoided antibody staining

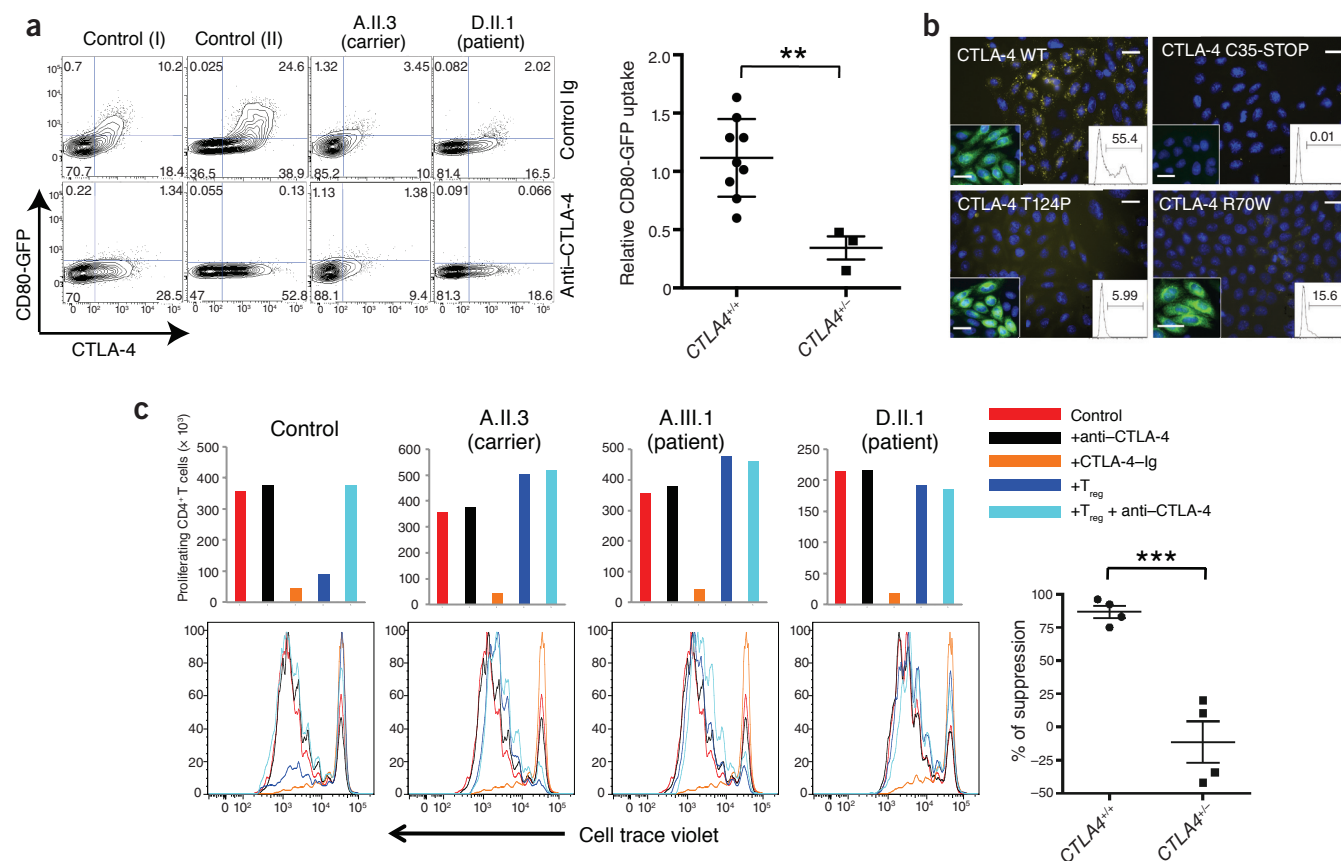


Figure 4 Impaired transendocytosis, ligand binding and T_{reg} suppressive activity in *CTLA4* heterozygotes. **(a)** Transendocytosis of CD80-GFP by stimulated primary CD4⁺FOXP3⁺ T_{reg} cells in the presence or absence of CTLA-4 blockade. Flow cytometry plots depict CD80-GFP uptake by T_{reg} cells in the absence (top) and presence (bottom) of CTLA-4 blockade. Dot plot shows the relative CD80-GFP uptake in homozygous versus heterozygous individuals ($P = 0.0091$). $n = 9$ *CTLA4*^{+/+}, $n = 3$ *CTLA4*^{+/-}. **(b)** Uptake of CD80-Ig (yellow) by CHO cells expressing wild-type and mutant *CTLA4*. Right insets, flow cytometric analysis of CD80-Ig staining in CHO cells (x axis, CD80-Ig staining; y axis, relative cell number). Left insets, CTLA-4 expression (green) in CHO cells, as assessed by staining with an antibody to the C terminus of CTLA-4. Images are representative of 4 independent experiments. Scale bars, 10 μ m. **(c)** Proliferation of cell trace-labeled CD4⁺ responder T cells upon coculture with monocyte-derived dendritic cells and CD3-specific antibodies with or without CD4⁺CD25⁺ T_{reg} cells, CTLA-4-Ig or CTLA-4-specific blocking antibodies. Quantification of total proliferating T cell numbers (top) and flow cytometry histograms depicting cell division of responder T cells in suppression assays (bottom). $n = 4$ *CTLA4*^{+/+}, $n = 4$ *CTLA4*^{+/-}. P values were determined by Student's t -test. ** $P < 0.01$, *** $P < 0.001$.

being compromised by the mutations in the extracellular domain (Fig. 4b). We detected full-length CTLA4 protein in cells transfected with the *CTLA4* mutants R70W (family C) and T124P (family D; Fig. 4b). In contrast, we found no protein expression in cells transfected with the C35* (family A) mutant, ruling out the use of an alternative start codon at Met38 immediately downstream of the premature stop codon. Cells transfected with either the T124P or the R70W mutant were impaired in their ability to take up soluble CD80-immunoglobulin fusion protein (CD80-Ig) (Fig. 4b). Thus, although these mutations are not within the known MYPPPY ligand-binding motif of CTLA-4 (ref. 31) (Supplementary Fig. 2), they appear to impair ligand binding and uptake.

CTLA4 mutations impair T_{reg} cell suppression

We tested the impact of *CTLA4* heterozygosity on regulatory T cell function *in vitro* using T cells and dendritic cells from healthy donors as targets for suppression. Under control conditions, naive CD4⁺ cells proliferated in response to CD3-specific antibodies and cocultured dendritic cells (Fig. 4c). Proliferation was CD80 and CD86 ligand-dependent, as it was inhibited by the addition of CTLA-4-Ig (abatacept; Fig. 4c). Addition of control T_{reg} cells from healthy donors efficiently

suppressed CD4⁺ T cell proliferation, and this was reversed by a CTLA-4-specific blocking antibody, indicating that the suppressive function of the T_{reg} cells in this assay is CTLA-4 dependent (Fig. 4c). T_{reg} cells from individuals with heterozygous *CTLA4* mutations were unable to suppress CD4⁺ T cell proliferation as compared to healthy *CTLA4*^{+/+} controls (Fig. 4c). These data reveal a defect in the CTLA-4-dependent suppressive activity of T_{reg} cells from individuals carrying heterozygous *CTLA4* mutations.

DISCUSSION

CD28 co-stimulation is required for T cell effector function and generation of T memory cells, and it also influences B cell class switching and T_{reg} cell homeostasis³². These processes are negatively regulated by CTLA-4. Interfering with the CD28-CTLA-4 pathway can therefore have both immune-stimulatory and immune-inhibitory effects³³⁻³⁵. Here, we report the phenotype of patients with previously undescribed heterozygous mutations in *CTLA4* providing clear evidence of its importance in immune homeostasis and T_{reg} cell suppressive function.

In families A, B and F, the *CTLA4* mutations most likely ablate CTLA-4 protein expression, rendering individuals haploinsufficient for CTLA-4. From these families, we learn that the gene dosage of *CTLA4*

is important, especially for the function of regulatory T cells. In families C–E, the mutations affect the ligand binding of CTLA-4, impairing the interaction of CTLA-4 with CD80 and CD86. As CTLA-4 forms homodimers and clusters with its ligands, these mutants may exert a dominant-negative effect.

Of 19 individuals with a proven heterozygous mutation in *CTLA4*, 12 presented with severe clinical manifestations. The availability of samples from currently healthy family members carrying the *CTLA4* mutation provided an opportunity to examine the consequences of this mutation in a setting uncoupled from illness or treatment. Notably, those individuals tested so far also exhibited a similar reduction in CTLA-4 expression, CTLA-4-dependent transendocytosis and T_{reg} cell suppressive function. This suggests that additional modifiers, including genetic, epigenetic or environmental factors, may exist that influence the clinical outcome of CTLA-4 deficiency³⁶. As the age of disease onset for clinical symptoms associated with CTLA-4 deficiency ranges in our patient cohort from 7 to 40 years, currently healthy, young mutation carriers may develop disease later. Indeed, autoimmune features (for example, psoriasis, type 1 diabetes and prolonged episodes of diarrhea) are evident in carriers previously classified as healthy (**Supplementary Table 1**). The breadth of autoimmune targets in patients and carriers is consistent with the range of autoimmunity reported in the setting of Foxp3 deficiency³⁷.

One notable finding is that patients with defects in CTLA-4 expression and function present with hypogammaglobulinemia in immunodeficiency clinics. Given that CTLA-4 inhibits the CD28 pathway, which plays a role in T cell help for B cell responses, deficiency in CTLA-4 might be expected to enhance CD28 function and promote humoral immunity. One possible explanation is that hyperactivation of T cells may result in infiltration and disruption of the bone marrow niche, impairing B cell development. This is consistent with the disruptions in B cell lymphopoiesis in T_{reg} cell-deficient mice³⁸. Alternatively, increased CD28-dependent follicular helper T cell differentiation³⁹ could result in chronic stimulation of B cells, leading to exhaustion. There may also be parallels with the phosphoinositide 3-kinase δ -activating mutations^{40,41} that cause defects in B cell class switching despite hyperactivation of T cell responses. As CD28 is a major phosphoinositide 3-kinase activator in T cells⁴², this link warrants future investigation.

Kuehn *et al.*⁴³ recently reported a group of patients with heterozygous *CTLA4* mutations. The clinical phenotype of their patients bears considerable similarity to those reported herein, and they also report incomplete penetrance of the disease phenotype, suggesting that CTLA-4 deficiency leads to a broad, yet well-defined, clinical syndrome. Our patient cohort contains different mutations from those of Kuehn *et al.*⁴³, suggesting there may be a spectrum of genetic alterations leading to defective CTLA-4 function. We have identified several point mutations in the ectodomain of the expressed CTLA-4 protein. Although we show in cellular assays that ligand binding to these mutants is impaired, it remains to be formally determined whether this impairment is solely due to changes in CTLA-4 affinity for its ligands or whether CTLA-4 structural stability is affected.

The binding of CTLA-4 to its ligands is closely coupled to its function as a competitor for CD28 co-stimulation. Accordingly, T_{reg} cell function, which requires the ability of CTLA-4 to bind to and remove its ligands from APCs, is impaired in individuals bearing *CTLA4* mutations. Given the key role of CTLA-4–ligand interactions, it is important in our view to study CTLA-4 in the context of CD80- or CD86-dependent T cell activation to probe its function. In this respect, although the defects in T_{reg} cell suppressive function in individuals with *CTLA4* mutations are consistent with those in Kuehn *et al.*⁴³, we did not observe any obvious alterations in conventional T cell proliferation (data not shown). There are numerous possible explanations for such differences; however, we

note their use of whole peripheral blood mononuclear cells (PBMCs) and stimulation with CD3-specific and CD28-specific antibodies⁴³. Given the enrichment of memory T cells in the patient samples, along with the presence of T_{reg} cells in these assays, it is unclear whether the hyperproliferative T cell phenotype reported is necessarily due to loss of CTLA-4 function in conventional T cells. The relative role of CTLA-4 in T_{reg} cells versus conventional T cells remains unclear, and additional work is needed to establish whether there is T cell–intrinsic hyperproliferation in patients bearing *CTLA4* mutations. In addition, whereas Kuehn *et al.*⁴³ report CTLA-4 expression on B cells, we were unable to detect CTLA-4 expression on B cells in the conditions we tested (**Supplementary Fig. 7**). Despite these differences in immunological detail, together our studies make a compelling argument that quantitative deficiencies in CTLA-4 protein expression predispose individuals to both autoimmunity and immunodeficiency.

Alterations in immune homeostasis are a feature of primary immunodeficiency, and organs with surfaces exposed to microbes, including the intestine, lungs and skin, seem to be particularly vulnerable to infections. The discovery of heterozygous loss-of-function mutations in *CTLA4* suggests that the CD28 and CTLA-4 pathway may be therapeutically targeted in selected subsets of patients with inflammatory bowel disease, enteropathy and wasting disease, granulomatous lung disease and autoimmune cytopenias. Soluble CTLA-4 fusion proteins (abatacept and belatacept), which bind to CD80 and CD86 and inhibit immune activation, have proven beneficial for the treatment of autoimmune disease and prevention of organ rejection^{35,44,45}. Whether they could be beneficial in the context of CTLA-4 deficiency warrants investigation.

METHODS

Methods and any associated references are available in the [online version of the paper](#).

Note: Any Supplementary Information and Source Data files are available in the online version of the paper.

ACKNOWLEDGMENTS

We thank the patients and their relatives for their participation in this study. We thank F. Atschekzei, S. Kock, A. Gaa, S. Glatzel and M. Stenzel for technical assistance, and D. Comtesse, R. Weinert, R. Wieland, M. Schüler and N. Verma for their excellent and dedicated patient care. This research was funded by the Bundesministerium für Bildung und Forschung with the following grants: Integriertes Forschungs- und Behandlungszentrum/Center for Chronic Immunodeficiencies 01EO1303, Systems Biology E:med/SysInflame: 012X1306F; the Deutsches Zentrum für Infektionsforschung #8000805-3 and in part by the Excellence Initiative of the German Research Foundation (GSC-4, Spemann Graduate School) and by the Intramural Research Program of the US National Institutes of Health, National Library of Medicine. We also thank the German Crohn's and Colitis Foundation for support of the exome sequencing and the Deutsche Forschungsgemeinschaft (DFG) Cluster of Excellence "Inflammation at Interfaces." B.A.G. is funded by the DFG CRC 992 Medical Epigenetics, L.S.K.W. by a UK Medical Research Council Senior Fellowship, T.Z.H. by the Wellcome Trust, R.K. by Diabetes UK, J.B.W. by a Japan Society for the Promotion of Science Young Scientist B grant and S.S. by the Ministry of Education, Culture, Sports, Science and Technology of Japan and the Japan Science and Technology Agency.

AUTHOR CONTRIBUTIONS

D.S. conceived and performed experiments, analyzed and interpreted the data, and co-wrote the manuscript. C.B. performed experiments and analyzed the data. R.K. designed and performed CTLA-4 staining and transendocytosis experiments, and analyzed the data. T.Z.H. designed and performed T_{reg} cell suppression assays, and analyzed the data. J.B.W. conceived and performed the mouse experiments, and interpreted the data. A.K. performed cloning, mutagenesis, transfection and microscopy. A.B., B.-S.P. and B.A.G. analyzed whole-exome sequencing data, A.A.S. analyzed the linkage analysis data, and S.U. performed experiments and analyzed the data. N.F. managed patients, and analyzed next-generation sequencing data. U.B., T.W., R.E.S., G.D., T.N., S. Seneviratne, M.K., C.S., S.E., R.T., P.H. and U.S. managed patients and provided the clinical data and patient's material, A.R.-E., K.W., M.R., F.E., T.C., R.B., P.F., M.S., A.M. and A.S.-G. designed and interpreted

experiments. S.I. performed crystallographic modeling. A.F. and S. Sakaguchi conceived, designed and interpreted experiments. L.S.K.W. and D.M.S. conceived, designed and interpreted experiments and co-wrote the manuscript. B.G. managed patients, conceived and interpreted experiments, and co-wrote the manuscript.

COMPETING FINANCIAL INTERESTS

The authors declare no competing financial interests.

Reprints and permissions information is available online at <http://www.nature.com/reprints/index.html>.

- Bacchetta, R. & Notarangelo, L.D. Immunodeficiency with autoimmunity: beyond the paradox. *Front. Immunol.* **4**, 77 (2013).
- Al-Herz, W. *et al.* Primary immunodeficiency diseases: an update on the classification from the international union of immunological societies expert committee for primary immunodeficiency. *Front. Immunol.* **5**, 162 (2014).
- Resnick, E.S. & Cunningham-Rundles, C. The many faces of the clinical picture of common variable immune deficiency. *Curr. Opin. Allergy Clin. Immunol.* **12**, 595–601 (2012).
- Yong, P.F., Thaventhiran, J.E. & Grimbacher, B. “A rose is a rose is a rose,” but CVID is Not CVID common variable immune deficiency (CVID), what do we know in 2011? *Adv. Immunol.* **111**, 47–107 (2011).
- Gathmann, B. *et al.* Clinical picture and treatment of 2212 patients with common variable immunodeficiency. *J. Allergy Clin. Immunol.* **134**, 116–126 (2014).
- Chen, K. *et al.* Germline mutations in NFKB2 implicate the noncanonical NF-kappaB pathway in the pathogenesis of common variable immunodeficiency. *Am. J. Hum. Genet.* **93**, 812–824 (2013).
- Jou, S.T. *et al.* Identification of variations in the human phosphoinositide 3-kinase p110delta gene in children with primary B-cell immunodeficiency of unknown aetiology. *Int. J. Immunogenet.* **33**, 361–369 (2006).
- Hori, S., Nomura, T. & Sakaguchi, S. Control of regulatory T cell development by the transcription factor Foxp3. *Science* **299**, 1057–1061 (2003).
- Kim, J.M., Rasmussen, J.P. & Rudensky, A.Y. Regulatory T cells prevent catastrophic autoimmunity throughout the lifespan of mice. *Nat. Immunol.* **8**, 191–197 (2007).
- Ochs, H.D., Ziegler, S.F. & Torgerson, T.R. FOXP3 acts as a rheostat of the immune response. *Immunol. Rev.* **203**, 156–164 (2005).
- Tivol, E.A. *et al.* Loss of CTLA-4 leads to massive lymphoproliferation and fatal multiorgan tissue destruction, revealing a critical negative regulatory role of CTLA-4. *Immunity* **3**, 541–547 (1995).
- Waterhouse, P. *et al.* Lymphoproliferative disorders with early lethality in mice deficient in Ctl4. *Science* **270**, 985–988 (1995).
- Fontenot, J.D., Gavin, M.A. & Rudensky, A.Y. Foxp3 programs the development and function of CD4+CD25+ regulatory T cells. *Nat. Immunol.* **4**, 330–336 (2003).
- Khattry, R., Cox, T., Yasayko, S.A. & Ramsdell, F. An essential role for Scurfin in CD4+CD25+ T regulatory cells. *Nat. Immunol.* **4**, 337–342 (2003).
- Friedline, R.H. *et al.* CD4+ regulatory T cells require CTLA-4 for the maintenance of systemic tolerance. *J. Exp. Med.* **206**, 421–434 (2009).
- Read, S., Malmstrom, V. & Powrie, F. Cytotoxic T lymphocyte-associated antigen 4 plays an essential role in the function of CD25(+)CD4(+) regulatory cells that control intestinal inflammation. *J. Exp. Med.* **192**, 295–302 (2000).
- Takahashi, T. *et al.* Immunologic self-tolerance maintained by CD25(+)CD4(+) regulatory T cells constitutively expressing cytotoxic T lymphocyte-associated antigen 4. *J. Exp. Med.* **192**, 303–310 (2000).
- Walker, L.S. Treg and CTLA-4: two intertwining pathways to immune tolerance. *J. Autoimmun.* **45**, 49–57 (2013).
- Wing, K. *et al.* CTLA-4 control over Foxp3+ regulatory T cell function. *Science* **322**, 271–275 (2008).
- Rudd, C.E. The reverse stop-signal model for CTLA4 function. *Nat. Rev. Immunol.* **8**, 153–160 (2008).
- Walker, L.S. & Sansom, D.M. The emerging role of CTLA4 as a cell-extrinsic regulator of T cell responses. *Nat. Rev. Immunol.* **11**, 852–863 (2011).
- Wing, K., Yamaguchi, T. & Sakaguchi, S. Cell-autonomous and -non-autonomous roles of CTLA-4 in immune regulation. *Trends Immunol.* **32**, 428–433 (2011).
- Bachmann, M.F., Kohler, G., Ecabert, B., Mak, T.W. & Kopf, M. Cutting edge: lymphoproliferative disease in the absence of CTLA-4 is not T cell autonomous. *J. Immunol.* **163**, 1128–1131 (1999).
- Homann, D. *et al.* Lack of intrinsic CTLA-4 expression has minimal effect on regulation of antiviral T-cell immunity. *J. Virol.* **80**, 270–280 (2006).
- Qureshi, O.S. *et al.* Trans-endocytosis of CD80 and CD86: a molecular basis for the cell-extrinsic function of CTLA-4. *Science* **332**, 600–603 (2011).
- Collins, A.V. *et al.* The interaction properties of costimulatory molecules revisited. *Immunity* **17**, 201–210 (2002).
- Bour-Jordan, H. & Bluestone, J.A. Regulating the regulators: costimulatory signals control the homeostasis and function of regulatory T cells. *Immunol. Rev.* **229**, 41–66 (2009).
- Keir, M.E. & Sharpe, A.H. The B7/CD28 costimulatory family in autoimmunity. *Immunol. Rev.* **204**, 128–143 (2005).
- Chambers, C.A. *et al.* The role of CTLA-4 in the regulation and initiation of T-cell responses. *Immunol. Rev.* **153**, 27–46 (1996).
- Schmidt, E.M. *et al.* Ctl4 controls regulatory T cell peripheral homeostasis and is required for suppression of pancreatic islet autoimmunity. *J. Immunol.* **182**, 274–282 (2009).
- Schwartz, J.C., Zhang, X., Fedorov, A.A., Nathenson, S.G. & Almo, S.C. Structural basis for co-stimulation by the human CTLA-4/B7-2 complex. *Nature* **410**, 604–608 (2001).
- Sansom, D.M. & Walker, L.S. The role of CD28 and cytotoxic T-lymphocyte antigen-4 (CTLA-4) in regulatory T-cell biology. *Immunol. Rev.* **212**, 131–148 (2006).
- Pardoll, D.M. The blockade of immune checkpoints in cancer immunotherapy. *Nat. Rev. Cancer* **12**, 252–264 (2012).
- Tabares, P. *et al.* Human regulatory T cells are selectively activated by low-dose application of the CD28 superagonist TGN1412/TAB08. *Eur. J. Immunol.* **44**, 1225–1236 (2014).
- Vincenti, F. *et al.* Costimulation blockade with belatacept in renal transplantation. *N. Engl. J. Med.* **353**, 770–781 (2005).
- Parkes, M., Cortes, A., van Heel, D.A. & Brown, M.A. Genetic insights into common pathways and complex relationships among immune-mediated diseases. *Nat. Rev. Genet.* **14**, 661–673 (2013).
- Barzaghi, F., Passerini, L. & Bacchetta, R. Immune dysregulation, polyendocrinopathy, enteropathy, x-linked syndrome: a paradigm of immunodeficiency with autoimmunity. *Front. Immunol.* **3**, 211 (2012).
- Riewaldt, J. *et al.* Severe developmental B lymphopoietic defects in Foxp3-deficient mice are refractory to adoptive regulatory T cell therapy. *Front Immunol.* **3**, 141 (2012).
- Walker, L.S. *et al.* Compromised OX40 function in CD28-deficient mice is linked with failure to develop CXC chemokine receptor 5-positive CD4 cells and germinal centers. *J. Exp. Med.* **190**, 1115–1122 (1999).
- Angulo, I. *et al.* Phosphoinositide 3-kinase delta gene mutation predisposes to respiratory infection and airway damage. *Science* **342**, 866–871 (2013).
- Lucas, C.L. *et al.* Dominant-activating germline mutations in the gene encoding the PI(3)K catalytic subunit p110delta result in T cell senescence and human immunodeficiency. *Nat. Immunol.* **15**, 88–97 (2014).
- Boomer, J.S. & Green, J.M. An enigmatic tail of CD28 signaling. *Cold Spring Harb. Perspect. Biol.* **2**, a002436 (2010).
- Kuehn, H.S. *et al.* Immune dysregulation in human subjects with heterozygous germline mutations in CTLA4. *Science* **345**, 1623–1627 (2014).
- Atzeni, F. *et al.* Long-term safety of abatacept in patients with rheumatoid arthritis. *Autoimmun. Rev.* **12**, 1115–1117 (2013).
- Wofsy, D., Hillson, J.L. & Diamond, B. Abatacept for lupus nephritis: alternative definitions of complete response support conflicting conclusions. *Arthritis Rheum.* **64**, 3660–3665 (2012).

ONLINE METHODS

Ethics approval. All individuals donated samples following informed written consent under local ethics board-approved protocols 239/99_BG, 251/13_KW, and 282/11_SE version 140023 (Ethik Kommission der Albert-Ludwigs-Universität Freiburg) and protocols #04/Q0501/119_AM03 for affected individuals, #07/H0720/182 for family members and #08/H0720/46 for healthy controls (Royal Free Hospital & Medical School Research Ethics Committee, London).

Linkage analysis. Genotyping of microsatellite markers across the autosomes was done as described by Braig *et al.*⁴⁶ in 2003. Of particular interest here, there were 28 markers genotyped across chromosome 2. The marker D2S1384 (Marshfield map 200.43cM, human genome build 37/hg19 205.2 Mbp) is close to *CTLA4* (204.7 Mbp). The flanking markers genotyped were D2S1391 (186.21 cM, 185.0 Mbp) and D2S2944 (210.43 cM, 214.6 Mbp). At these markers, 15 family members were genotyped, including five individuals who were affected or obligate carriers. LOD scores were computed using FASTLINK^{47–49}.

Whole-exome sequencing. Exome sequencing was performed for all 14 available individuals of the pedigree. The samples were enriched using the TruSeq Exome Enrichment Kit (Illumina). Sequencing of 2 × 100 bp paired-end reads was performed for one quarter lane per sample on the Illumina HiSeq2000. The reads were mapped against the human reference genome build hg19 using BWA⁵⁰ v0.7.9, sorted, converted to bam format and indexed with SAMtools⁵¹ v0.1.17, followed by the removal of PCR duplicates with Picard v1.115 (<http://broadinstitute.github.io/picard/>). Local realignment around InDels and base quality score recalibration, as well as variant calling and variant quality score recalibration, were performed with the GATK⁵² v2.8 according to their best-practice recommendations. For annotation and predicting the effects of single nucleotide polymorphisms, we applied SnpEff and SnpSift v3.6 (<http://snpeff.sourceforge.net/>)⁵³. Work with genetic variation data in the form of VCF files was conducted using the VCFtools program package⁵⁴.

Genes were designated as related to the immune system using IRIS list⁵⁵ and GO list. The GO list was generated by composing the genes annotated in Gene Ontology⁵⁶ direct and indirect with the term “immune system process” (GO:0002376), defined as “Any process involved in the development or functioning of the immune system, an organismal system for calibrated responses to potential internal or invasive threats” (<http://amigo.geneontology.org/amigo/term/GO:0002376>).

Immunohistochemistry. Bone marrow biopsies were decalcified in EDTA before paraffin embedding. 3-µm sections were cut from formalin-fixed, paraffin-embedded samples. Upper gastrointestinal biopsies were routinely stained with hematoxylin and eosin stain and periodic acid–Schiff stain. Bone marrow biopsies were routinely stained with naphthol AS-D chloroacetate esterase (NASDCL). Immunohistochemical staining was performed using a horseradish peroxidase-catalyzed brown chromogen reaction together with ready-to-use antibodies in an automated staining system (Dako Autostainer Link; Dako, Glostrup, Denmark) following the manufacturer's guidelines. Depending on the tissue section size, up to three droplet zones are stained with 100 µl antibody solution per droplet zone. Antibodies to the following proteins were used (undiluted): CD3 (rabbit polyclonal, Dako), CD4 (clone 4B12, Dako), CD8 (clone C8/144B, Dako), CD19 (clone LE-CD19, Dako), CD20 (clone L26, Dako), CD38 (clone SPC 32, Novocastra, Newcastle upon Tyne, UK) and IgM, IgG and IgA (rabbit polyclonal antibodies; Dako). Photos were taken on an Olympus BX51 microscope (Olympus Germany, Hamburg, Germany) with the AxioCam MRC camera (Zeiss, Jena, Germany).

Flow cytometry. Peripheral blood mononuclear cells (PBMCs) were isolated through a Ficoll step gradient and stained for cell surface markers with fluorochrome-conjugated antibodies to the following proteins (dilutions indicated): CD38 1:100 (HIT-2, BD), IgD 1:500 (IA6-2, BD), IgM 1:80 (MHM-88, BioLegend), CD10 1:20 (HI10a, BD), CD19 1:100 (SJ25C1, BD), CD21 1:40 (B-ly4, BD), CD27 1:50 (0323, eBioscience), CD138 1:20 (B-B4, AbD Serotec), IgG 1:600 (SouthernBioTech #2043-09), IgA 1:50 (G20-359, BD), CD3 1:50 (SK7, BD), CD28 1:20 (CD28.2, BD), FOXP3 1:30 (PCH101, eBioscience), CD8 1:10 (SK1, BD), CD4 1:100 (RPA-T4, eBioscience), γδ-TCR 1:200 (B1.1, eBioscience), αβ-TCR 1:200 (IP26, eBioscience), CD45RO 1:50 (UCHL1, BD), CD45RA

1:100 (HI100, BD), CD57 1:20 (NK-1, BD), CD31 1:200 (WM59, eBioscience), CD62L 1:200 (DREG-56, BD), CD152/CTLA4 1:30 (BNI3, BD). Samples were acquired on a FACS-Canto II flow cytometer (BD) or on a Gallios flow cytometer (Beckman Coulter, Miami, FL) and analyzed using FlowJo version 7.6.5 analysis software (Treestar, Ashland, OR).

Cytokine expression by T cells. One million freshly isolated PBMCs were incubated overnight at 37 °C, 5% CO₂ in Iscove's Modified Dulbecco's Medium (GIBCO) supplemented with 10% FCS (GIBCO) and 1% penicillin/streptomycin (GIBCO) in a 96-well plate. Cells were then treated with GolgiPlug (BD) to inhibit intracellular protein transport and stimulated with 50 units/ml IL-2 (Novartis), PMA (0.05 µg/ml) and ionomycin (1 µg/ml) for 4 h at 37 °C, 5% CO₂. Subsequently, cells were stained for surface markers CD3 1:50 (SK7, BD), CD4 1:40 (SFC12T4D11, Beckman Coulter) and CD45RO 1:50 (UCHL1, BD) and intracellular markers IL-17 1:200 (eBio64DEC17, eBioscience), IL-4 1:20 (8D4-8, eBioscience) and IFN-γ 1:400 (B27, BD) and measured by flow cytometry. CD3⁺CD4⁺CD45RO⁺ cells were analyzed for cytokine expression levels.

TCR spectratyping and rearrangement studies. TCRβ, TCRγ and TCRδ spectratyping was performed from RNA following synthesis of oligo dT-primed cDNA as described⁵⁷. In order to study TCR rearrangements, DNA was amplified by PCR using the Biomed-2 primers and protocols⁵⁸. All fluorescent fragments were analyzed on an ABI 3130-XL capillary sequencer (Life Technologies, Darmstadt, Germany).

CTLA-4 staining in activated T_{reg} cells. 200,000–300,000 PBMCs (freshly isolated or frozen samples) were incubated overnight and then cultured for 16 h in the presence or absence of CD3/CD28 beads (Dynabeads Human T-Activator CD3/CD28) at a concentration of 1:1 (beads to cells). Cells were then stained for surface markers CD4 1:100 (RPA-T4, BD Bioscience), CD45RA 1:100 (HI100, eBioscience), CD127 1:10 (HIL-7R-M21, BD Bioscience) and CD25 1:10 (2A3, BD Bioscience), fixed, permeabilized and stained for FOXP3 1:30 (236A/E7, eBioscience) and CD152/CTLA-4 1:30 (BNI3, BD), before being assessed using a BD Canto II flow cytometer.

Mice. Heterozygous *Ctla4*-deficient (*Ctla4*^{+/-}) mice and wild-type (WT) littermates on a C57BL/6 background were maintained under specific pathogen-free conditions and used in experiments between 6–10 weeks of age; matched numbers of male and female mice were used. Required sample sizes were estimated on the basis of prior experience of animal studies. Experiments were conducted in compliance with Osaka university regulations, under protocols approved by the Animal Experiment Committee of Osaka University. No formal randomization or blinding was used. Groups used in experiments were age and sex matched, and no exclusion criteria were used. C57BL/6 *Ctla4*^{+/-} or WT littermates were vaccinated intraperitoneally with 100 µg 4-hydroxy-3-nitrophenylacetyl-ovalbumin (NP-OVA) at a molar ratio of 16 NP to 1 OVA in alum. Splenocytes were isolated by manual disaggregation with frosted slides and analyzed *ex vivo* on day 14 after immunization. Intracellular staining was carried out using the eBioscience FOXP3 staining buffer kit according to the manufacturer's instructions. Antibody clones were as follows: anti-B220: RA3-6B2, anti-CD4: RM4-5 (BD), anti-Foxp3: FJK-16s, anti-CD44: IM7, anti-CTLA-4 UC10-4B9 (Biolegend). Antibody dilutions were 1:200, except Foxp3 and CTLA-4 at 1:100. Dead cell discrimination was based on positivity for IR Live/Dead at a 1:250 dilution (Invitrogen). CTLA-4 and FoxP3 analysis was carried out on groups of between 4 and 13 mice. Data points in **Supplementary Fig. 5** represent individual mice.

Transendocytosis assays. Primary human CD4⁺ T cells were purified from whole PBMCs using EasySep Human CD4⁺ T Cell Enrichment Kit (Stemcell Tech.) and activated with CD3/CD28 beads for 16 h in the presence of CHO cells expressing CD80-GFP. CHO-K1 cells were obtained European Collection of Cell Cultures (ECACC) and were tested negative for mycoplasma. After 16 h, CTLA-4 expression (anti-CTLA-4-PE, BNI3, BD bioscience) was assessed by staining cells at 37 °C for the final 2 h. Subsequently, cells were stained for CD4 (RPA-T4, BD Bioscience, 1:50), CD45RA (HI100, eBioscience, 1:200), CD127 (HIL-7R-M21, BD Bioscience, 1:50) and CD25 (2A3, BD bioscience, 1:50) fixed and permeabilized and then stained for FOXP3 (236A/E7, eBioscience, 1:50). Cells were gated on FOXP3⁺ cells and analyzed for GFP uptake.

Human T_{reg} suppression assays. To study CTLA-4–dependent T_{reg} suppression, conditions were established where stimulation of responder T cells (by DCs plus anti-CD3) was shown to be sensitive to blockade by abatacept (CTLA-4-Ig). This ensures that the response is sensitive to the presence of CD80 and CD86 ligands on the APC and thereby sensitive to ligand removal by CTLA-4–expressing T_{reg} cells. In our experience, T cell responses that are not abatacept sensitive such as those stimulated using antibody-coated beads cannot be suppressed in a CTLA-4–dependent manner by T_{reg} cells. To perform such assays, freshly isolated resting CD4⁺ naïve T cells were washed with PBS and incubated with CellTrace Violet according to the manufacturer's instructions (Molecular Probes). The reaction was quenched with media containing serum followed by PBS wash, and cells were suspended at 1.8×10^6 cells/ml before use as responder T cells. T cell proliferation assays were performed in 250 μ l RPMI 1640 culture media. Responder T cells (0.9×10^5) were stimulated with 0.5 μ g/ml CD3-specific antibody (OKT3-ATCC). To provide co-stimulation, monocyte-derived DCs expressing CD80 and CD86 were used. To generate these, monocytes (2×10^6 cells/ml) were cultured in RPMI 1640 medium containing 10% FCS and antibiotics with GM-CSF (PeproTech, 800 U/ml) and IL-4 (PeproTech, 500 U/ml) for 5–7 d. DCs were present at a ratio of 1:10, DC to T cell. Cells were cultured for 5 d in the presence or absence of 10 μ g/ml CTLA-4-Ig (abatacept) or anti-CTLA-4 (20 μ g/ml). To measure T_{reg} suppression, unlabeled negatively selected CD4⁺CD25⁺ T_{reg} (2 T_{reg} cells to 1 DC) were added. Division of responder T cells was measured by the dilution of violet dye using flow cytometry. Live proliferating T cell counts were performed using counting beads (Dako) and analyzed using FlowJo software.

Statistical analyses. Unless otherwise indicated, statistical analysis was performed using GraphPad Prism version 6, and *P* values were calculated by two-

tailed unpaired Student's *t*-test for the means with a 95% confidence interval. In **Supplementary Figure 5**, a two-sided Mann-Whitney *U* test was performed.

46. Braig, D.U. *et al.* Linkage of autosomal dominant common variable immunodeficiency to chromosome 5p and evidence for locus heterogeneity. *Hum. Genet.* **112**, 369–378 (2003).
47. Cottingham, R.W. Jr., Idury, R.M. & Schaffer, A.A. Faster sequential genetic linkage computations. *Am. J. Hum. Genet.* **53**, 252–263 (1993).
48. Lathrop, G.M. & Lalouel, J.M. Easy calculations of lod scores and genetic risks on small computers. *Am. J. Hum. Genet.* **36**, 460–465 (1984).
49. Schäffer, A.A., Gupta, S.K., Shriram, K. & Cottingham, R.W. Jr. Avoiding recomputation in linkage analysis. *Hum. Hered.* **44**, 225–237 (1994).
50. Li, H. & Durbin, R. Fast and accurate short read alignment with Burrows-Wheeler transform. *Bioinformatics* **25**, 1754–1760 (2009).
51. Li, H. *et al.* The Sequence Alignment/Map format and SAMtools. *Bioinformatics* **25**, 2078–2079 (2009).
52. McKenna, A. *et al.* The Genome Analysis Toolkit: a MapReduce framework for analyzing next-generation DNA sequencing data. *Genome Res.* **20**, 1297–1303 (2010).
53. Cingolani, P. *et al.* A program for annotating and predicting the effects of single nucleotide polymorphisms, SnpEff: SNPs in the genome of *Drosophila melanogaster* strain w1118; iso-2; iso-3. *Fly (Austin)* **6**, 80–92 (2012).
54. Danecek, P. *et al.* The variant call format and VCFtools. *Bioinformatics* **27**, 2156–2158 (2011).
55. Abbas, A.R. *et al.* Immune response in silico (IRIS): immune-specific genes identified from a compendium of microarray expression data. *Genes Immun.* **6**, 319–331 (2005).
56. Ashburner, M. *et al.* Gene ontology: tool for the unification of biology. The Gene Ontology Consortium. *Nat. Genet.* **25**, 25–29 (2000).
57. Ehl, S. *et al.* A variant of SCID with specific immune responses and predominance of gamma delta T cells. *J. Clin. Invest.* **115**, 3140–3148 (2005).
58. van Dongen, J.J. *et al.* Design and standardization of PCR primers and protocols for detection of clonal immunoglobulin and T-cell receptor gene recombinations in suspect lymphoproliferations: report of the BIOMED-2 Concerted Action BMH4-CT98-3936. *Leukemia* **17**, 2257–2317 (2003).